Case Studies in Thermal Engineering 28 (2021) 101378

Contents lists available at ScienceDirect

Case Studies in Thermal Engineering

journal homepage: www.elsevier.com/locate/csite

Heat transfer and pressure drop in turbulent nanofluid flow in a pin-fin heat sink: Fin and nanoparticles shape effects

Yacine Khetib [a,b,*], Khaled Sedraoui [c], Ammar A. Melaibari [a,d], Ali Alzaied [e], Radi Alsulami [a], Mohsen Sharifpur [f,g,**]

[a] Mechanical Engineering Department, Faculty of Engineering, King Abdulaziz University, Jeddah, 80204, Saudi Arabia
[b] Center Excellence of Renewable Energy and Power, Jeddah, 80204, Saudi Arabia
[c] Faculty of Engineering, and Center of Research Excellence in Renewable Energy and Power Systems, King Abdulaziz University, Jeddah, Saudi Arabia
[d] Center of Nanotechnology, King AbdulAziz University, Jeddah, 80204, Saudi Arabia
[e] Architectural Engineering Department., Faculty of Engineering, Taif University, Taif, Saudi Arabia
[f] Department of Mechanical and Aeronautical Engineering, University of Pretoria, Pretoria, 0002, South Africa
[g] Department of Medical Research, China Medical University Hospital, China Medical University, Taichung, Taiwan

ARTICLE INFO

Keywords:
Heatsink
Nanoparticle shape
Pin shape
Turbulent flow

ABSTRACT

In this paper, the turbulent flow of a nanofluid in a channel is simulated in the presence of a pin-fin heatsink. Pin fins have different shapes, including hexagonal, circular, square, and triangular that are considered in two different arrangements. Constant heat flux is applied to the heatsink from its bottom due to the operation of an electronic chip. The nanoparticles suspended in water are alumina, which are in different shapes such as blades, bricks, cylinders, and plates. Their shape effect is investigated. The nanofluid enters the channel at a constant velocity in the range of 1–3 m/s and a constant volume percentage of 2%, and exits after cooling the pin-fin heatsink. The standard k-ε turbulence model is used to model turbulent flow, and the SIMPLEC method is employed to linearize the equations. The variables include fin type, fin arrangement, nanoparticle shape, and nanofluid velocity. Their effect on the maximum and average heatsink temperature and pressure drop (ΔP) is studied. The results show that increasing the velocity leads to a reduction in heatsink temperature, and the use of brick-shaped nanoparticles and circular fin results in the best cooling performance. Also, the use of circular fin and brick nanoparticles requires less ΔP than other cases.

1. Introduction

One of the major concerns in electronics systems is the heat generated by electronic devices. Various electronic devices produce heat during their operation and power consumption [1,2]. If they are not cooled, they may be seriously damaged or even burned [3,4]. Various devices such as heatsinks, microchannels, and other similar devices are employed for cooling electronic devices and chips. The heat generated by these devices has increased, and as a result, they need more cooling [5,6]. Small dimensions and lack of space for installing large parts have made it necessary to reject large heat in a small space. It is necessary to fabricate new heatsinks with higher

* Corresponding author. Mechanical engineering Department, Faculty of Engineering, King Abdulaziz University, Jeddah, 80204, Saudi Arabia.
** Corresponding author. Department of Medical Research, China Medical University Hospital, China Medical University, Taichung, Taiwan.
E-mail addresses: ykhetib@yahoo.com (Y. Khetib), mohsen.sharifpur@up.ac.za (M. Sharifpur).

https://doi.org/10.1016/j.csite.2021.101378
Received 14 May 2021; Received in revised form 13 August 2021; Accepted 22 August 2021
Available online 24 August 2021

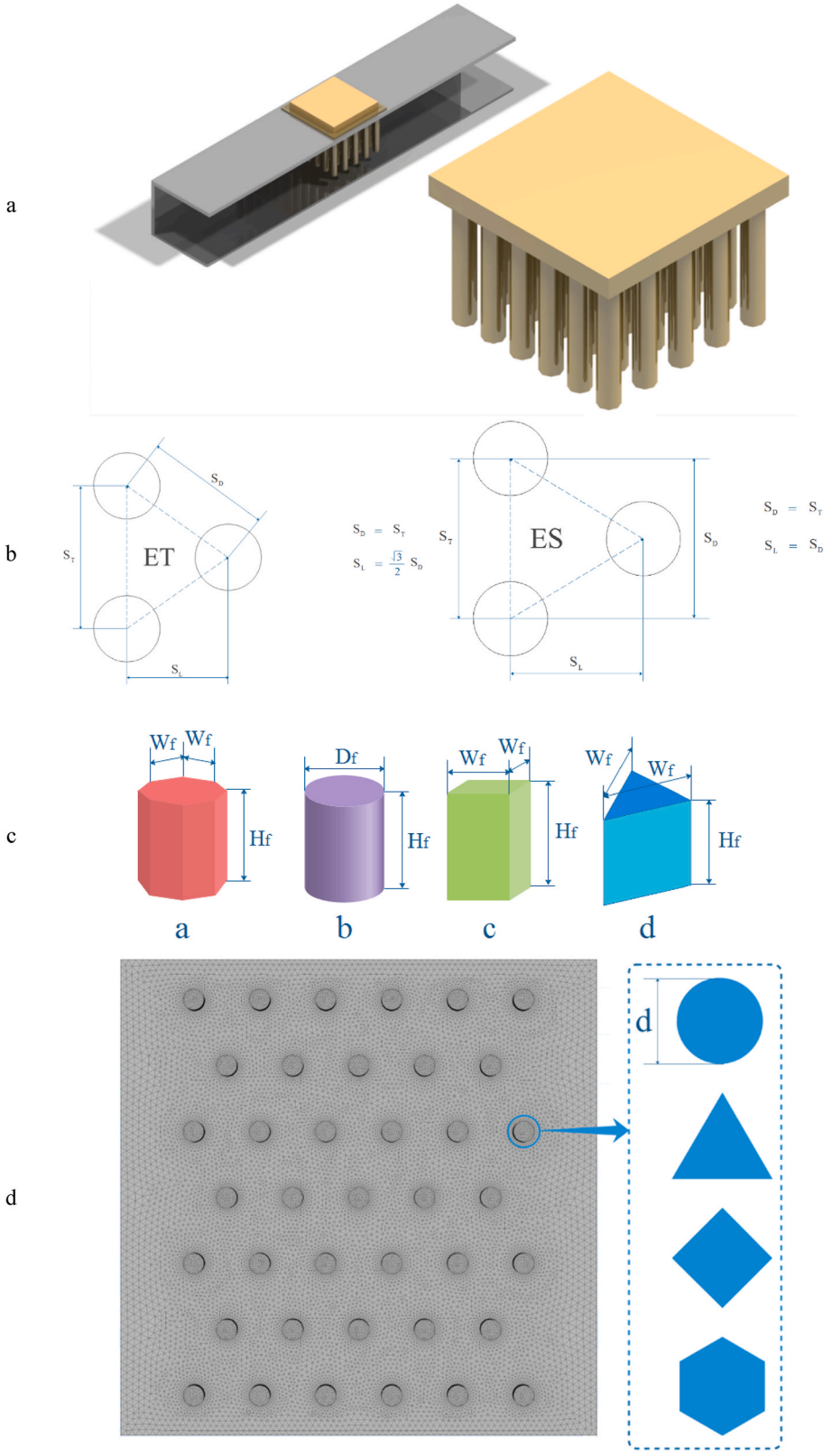

Fig. 1. Schematic of the problem.

performance. Many researchers have studied different types of heatsinks and have tried to produce heatsinks with higher performance [7,8]. Entropy generation (S_{gen}) in various devices indicates the energy loss amount in them. By examining the amount of S_{gen} in different devices, information can be obtained about the amount of losses. Various researchers have considered the rate of S_{gen} by different thermal devices [9–14]. Meanwhile, the study of S_{gen} can also help to better investigate heatsink. Evaluation of S_{gen} shows how much irreversibility and energy loss occur in different devices [15–18]. In one of these articles, Shahsavar et al. [19] studied a micro-heatsink with one input and four outputs and considered S_{gen}. Their findings revealed that increasing the Reynolds number diminishes the heatsink temperature. They demonstrated that the addition of nanoparticles does not affect heatsink temperature. It was found that thermal S_{gen} decreases with the Reynolds number. However, the addition of nanoparticles is more effective on thermal S_{gen} at higher Reynolds numbers and has a decreasing effect on it at higher Reynolds numbers.

One of the most widely used types of heatsinks is the pin-fin heatsink. In this type of heatsink, fins in the form of the pin are placed in the cooling fluid flow path to cool the device properly. Researchers have studied this type of heatsink in the last years [20–25]. Hassan [26] studied the heat transfer rate (HTR) of nanofluids inside a micro-fin pin numerically. The variables in his paper included square, circular, and triangular pins and diamond-water and water-alumina nanofluids. The three-dimensional simulation was performed using the FVM. His results showed that the use of nanofluids for all pin-fin geometries improves the HTR. Diamond-water nanofluids showed better thermal performance than water-alumina one. It was shown that the amount of HTR and the ΔP increase with the volume percentage of nanoparticles. Ambreen et al. [27] examined the influence of fin geometry and nanofluids on the heat transfer of heatsinks. Their results showed that nanofluids improve the heatsink performance. The amount of HTR from high to low was related to the circular, square, and triangular shapes of fins, respectively. When HTR increases, the ΔP is enhanced.

A heatsink can be cooled with various fluids. The most common of which are water and air, which are widely used. Other types of fluid that have good cooling ability, according to previous studies are nanofluids. Nanofluids have been used in various articles as a cooling and heat transfer fluid [28–31]. This type of fluid that has been considered by many researchers in the last two decades has a good cooling ability and has been used for cooling heatsinks [32–34]. Nanoparticles can be prepared using different methods. The nanoparticles have different thermal conductivity and change the fluid viscosity. These researchers have also investigated the influence of nanoparticles shape on HTR [35–39]. For instance, Arani et al. [40] considered the effect of dissimilar nanoparticles on the thermal efficiency of a microchannel. Their results showed that the use of cylindrical nanoparticles has the best HTR and thermal efficiency among nanoparticles. Bahiraei et al. [41] evaluated the irreversibility of various nanofluids in a heatsink numerically. Their results showed that plate-shaped nanoparticles produce the lowest thermal S_{gen}. While this type of nanoparticle leads to the highest S_{gen} due to viscous dissipation. The minimum total S_{gen} also belongs to the plate-shaped nanoparticles. It was also demonstrated that the rate of thermal S_{gen} is much higher than the one due to viscous dissipation.

The use of heatsinks for cooling various devices is very common. Thus, numerous investigations have been carried out in the field of heatsinks. Pin-fin heat sinks have attracted the attention of many researchers. The use of different types of pins can improve the thermal performance of heatsinks. Also, the use of nanofluids helps affect the HTR. Through comparing different pin fin structure, the usefulness of each shape is challenged. In this paper, the effect of different nanoparticle shapes as well as different pinfin shapes on heatsink performance in two different configurations is investigated.

2. Problem statement and governing equations

A heatsink located inside a channel in which nanofluid flows is employed for cooling an electronic chip, as shown in Fig. 1a. This heatsink has several pin fins. The fluid passes through the pin fins and cools them. The electronic chip is heated due to its operation and generates a constant heat flux of 100 W/m^2. The dimensions of the heatsink and its other geometry details are shown in Fig. 1a. The nanofluid stream enters the channel with uniform velocity and temperature. The fully developed fluid flow exits the channel with a constant pressure boundary condition. Also, all parts except the area that has been subjected to heat flux are well insulated. Besides, a no-slip boundary condition is imposed on the walls. Pin fins can have two different arrangements. The arrangements, i.e. ES and ET, and the distance between pin fins are illustrated in Fig. 1b.

Table 1 Shows the dimensions of channel and pin fin for dissimilar arrangements of pins.

Pin fin can also have many shapes. The shapes studied in this paper include triangular, square, hexagonal, and circle, which is shown in Fig. 1c. Moreover, in Fig. 1d, the layout of each fin is illustrated. In the following, the effect of using each shape of pin fin will be evaluated.

According to the following assumptions, the governing equations are expressed as Eqs. (1)–(6):

- The flow is turbulent incompressible.
- The nanofluid flow is homogeneous and single phase.
- The acceleration of gravity and natural convection and radiation HTR is neglected.
- Thermal effect due to viscosity is negligible.

$$\frac{\partial U}{\partial X}+\frac{\partial V}{\partial Y}+\frac{\partial W}{\partial Z}=0 \tag{1}$$

$$U\frac{\partial U}{\partial X}+V\frac{\partial U}{\partial Y}+W\frac{\partial U}{\partial Z}=-\frac{1}{\rho_f}\frac{\partial P}{\partial X}+\frac{\mu_f}{\rho_f}\left(\frac{\partial^2 U}{\partial X^2}+\frac{\partial^2 U}{\partial Y^2}+\frac{\partial^2 U}{\partial Z^2}\right) \tag{2}$$

Table 1
Dimensions of channel and pin fin for dissimilar arrangements of pins.

	d	h	S_L	S_D	S_T
ES	1–5	1–5	8	8	8
ET	1–5	1–5	7.794	9	9

$$U\frac{\partial V}{\partial X}+V\frac{\partial V}{\partial Y}+W\frac{\partial V}{\partial Z}=-\frac{1}{\rho_f}\frac{\partial P}{\partial Y}+\frac{\mu_f}{\rho_f}\left(\frac{\partial^2 V}{\partial X^2}+\frac{\partial^2 V}{\partial Y^2}+\frac{\partial^2 V}{\partial Z^2}\right) \tag{3}$$

$$U\frac{\partial W}{\partial X}+V\frac{\partial W}{\partial Y}+W\frac{\partial W}{\partial Z}=-\frac{1}{\rho_f}\frac{\partial P}{\partial Z}+\frac{\mu_f}{\rho_f}\left(\frac{\partial^2 W}{\partial X^2}+\frac{\partial^2 W}{\partial Y^2}+\frac{\partial^2 W}{\partial Z^2}\right) \tag{4}$$

$$\left(U\frac{\partial T_f}{\partial X}+V\frac{\partial T_f}{\partial Y}+W\frac{\partial T_f}{\partial Z}\right)=\frac{1}{\alpha_f}\left(\frac{\partial^2 T_f}{\partial X^2}+\frac{\partial^2 T_f}{\partial Y^2}+\frac{\partial^2 T_f}{\partial Z^2}\right) \tag{5}$$

$$0=k_s\left(\frac{\partial^2 T_s}{\partial X^2}+\frac{\partial^2 T_s}{\partial Y^2}+\frac{\partial^2 T_s}{\partial Z^2}\right) \tag{6}$$

references [23,42,43] used the standard k-ε turbulence model to simulate the cooling of the pin fin heatsink at low fluid velocity. Due to the low-velocity turbulence flow, the standard k-ε model is also employed in the present simulations. Comparison between the k-ε and k-ω SST has been done to simulate pin fin heatsinks [44] and they indicated that there is no difference between the two equations. Hence, the standard k-ε turbulence model is applied in the present study:

$$\frac{\partial(U\rho k)}{\partial X}=\frac{\partial}{\partial X}\left[\left(\mu+\frac{\mu_t}{\sigma_k}\right)\frac{\partial k}{\partial X}\right]+\mu_t\left(\frac{\partial V}{\partial X}+\frac{\partial U}{\partial Y}\right)\frac{\partial V}{\partial X}-\rho\varepsilon \tag{7}$$

$$\frac{\partial(U\rho\varepsilon)}{\partial X}=\frac{\partial}{\partial X}\left[\left(\mu+\frac{\mu_t}{\sigma_\varepsilon}\right)\frac{\partial \varepsilon}{\partial X}\right]+C_1\frac{\varepsilon}{k_f}\mu_t\left(\frac{\partial V}{\partial X}+\frac{\partial U}{\partial Y}\right)\frac{\partial V}{\partial X}-\rho C_2\frac{\varepsilon^2}{k_f} \tag{8}$$

Note that $\varepsilon = 1.3$, $k = 1$.

3. Boundary conditions and numerical method

The boundary conditions of the problem can be defined according to Fig. 1a as follows:
1-Channel inlet (uniform flow):

$U = U_{In}$	$W = V = 0$	$T = T_{In} = 293.15$

2-Channel output (fully developed flow):

$\frac{\partial U}{\partial X} = 0$	$W = V = 0$	$\frac{\partial T}{\partial X} = 0$

3- Heatsink to pin fins (thermal conductivity and no-slip boundary condition):

$U = W = V = 0$	$T_l = T_S$	$-k_l\frac{\partial T}{\partial n} = k_S\frac{\partial T}{\partial n} = 0$

In these relationships, the indices l and s refer to the working fluid and the solid, respectively.
4-Channel walls (no-slip and insulated):

$U = W = V = 0$	$-k_l\frac{\partial T}{\partial n} = 0$

At the top of the heatsink wall, constant heat flux is applied.
Finally, the geometry has meshed, and then the governing equations are solved numerically using the above boundary conditions.

Table 2
Values of constants for different nanoparticle shapes of Al_2O_3 nanoparticles [45].

	C_k	A_1	A_2
Platelets	2.61	37.1	612.6
Blades	2.74	14.6	123.3
Cylinders	3.95	13.5	904.4
Bricks	3.37	1.9	471.4

Table 3
Thermophysical properties of water and nanoparticles.

Properties	C_P (J /kg.K)	k (w /m.K)	ρ (kg /m^3)	μ (kg /m.s)
Water	4179	0.613	997.1	0.001
AlOOH	618.3	30	6050	–

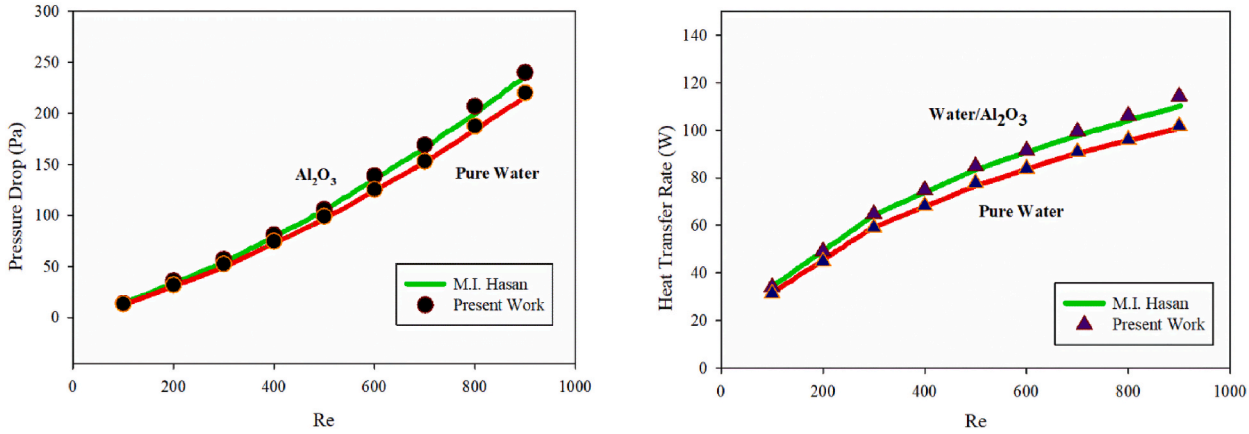

Fig. 2. ΔP and HTR obtained from the present simulations and Hasan et al. [26].

Table 4
Grid independence test.

ES			
	h	ΔT	ΔP
Mesh1(Size 0.0003)	2367828	312.988	23042
Mesh2(Size 0.0002)	2201652	312.420	22958
Mesh3(Size 0.0001)	2171797	311.590	22450
Mesh4(Size 0.00009)	2170792	311.592	22458
ET			
	h	ΔT	ΔP
Mesh1(Size 0.0003)	2101767	311.482	20042
Mesh2(Size 0.0002)	2097453	310.42	19458
Mesh3(Size 0.0001)	2066779	309.221	19337
Mesh4(Size 0.00009)	2066772	309.225	19330

The SIMPLEC algorithm is used to couple the velocity and pressure fields in the momentum equation. The findings for the velocity equations are solved in 3-dimension with a convergence coefficient of $10^{-4,}$ and the energy equation is resolved with a convergence coefficient of 10^{-6}.

4. Nanofluid properties

Nanofluid properties including density and specific heat are defined as follows:

$$\rho_{nf} = \phi\rho_p + (1-\phi)\rho_f \tag{9}$$

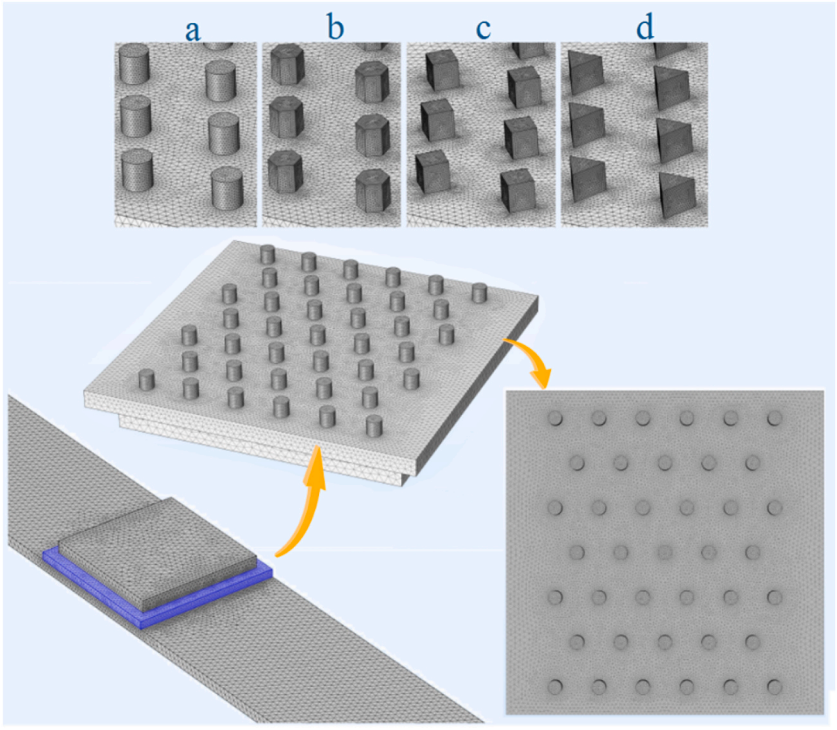

Fig. 3. The grid used for different shapes of pin fin.

$$c_{p,nf} = \frac{(1-\phi)(\rho c_p)_f + \phi(\rho c_p)_p}{\rho_{nf}} \tag{10}$$

where p represents nanoparticles and the f indicates water to investigate the effect of nanoparticle shape that are proposed by Timofeeva et al. [45] who investigated the influence of dissimilar nanoparticle shapes of alumina boehmite nanoparticles. Their proposed relationships are as follows:

$$\frac{k_f}{k_{bf}} = 1 + C_k\phi \tag{11}$$

$$\frac{\mu_f}{\mu_{bf}} = 1 + A_1\phi + A_2\phi^2 \tag{12}$$

where ϕ is the volume percentage of nanoparticles and constants C_k, A_1, and A_2depend on the shape of nanoparticles (Table 2).

Table 3 Shows the thermophysical properties of water and nanoparticles.

5. Data acquisition

Two important parameters in the study of pin fin structure are their hydraulic and thermal performance. The amount of heat in the heatsink is obtained as follows:

$$Q = \dot{m}C_{pf}(T_{Out} - T_{In}) \tag{13}$$

On the other hand, the convective heat transfer coefficient (h) is written as follows

$$h = \frac{Q}{A_S\left[T_w - \frac{T_{Out}+T_{In}}{2}\right]} \tag{14}$$

where $A_S$is the surface area of the heatsink plate and T_w is the average pin fin temperature. The pressure drop in the channel is as follows:

$$\Delta P = \overline{P}_{Inlet} - \overline{P}_{Outlet} \tag{15}$$

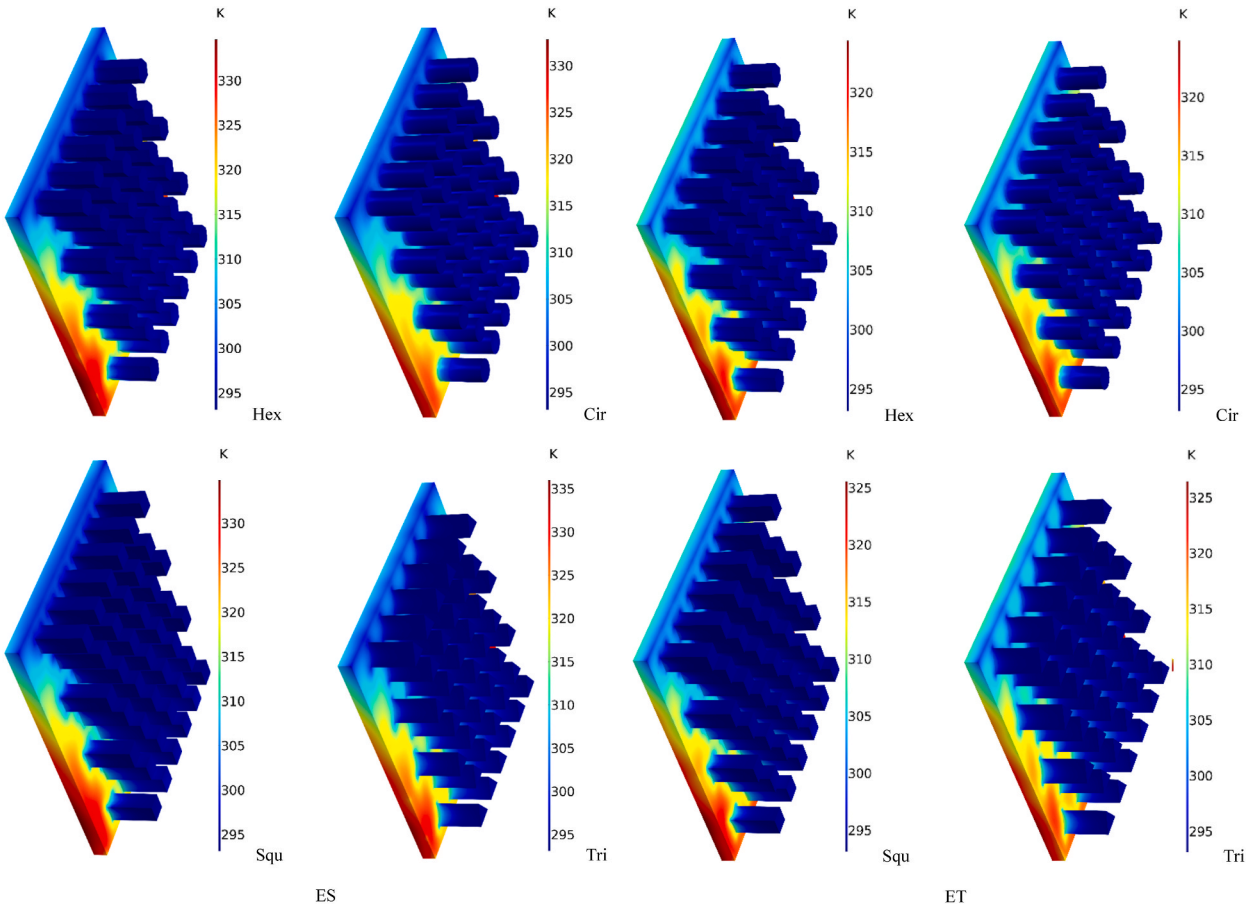

Fig. 4. Temperature contours on the heatsink for two pin-fin arrangements for different shapes of the pin and blade-shaped nanoparticles and the inlet velocity of 2 m/s.

where $\overline{P}_{Inlet}$ and $\overline{P}_{Outlet}$ represent the inlet and outlet pressure, respectively.

6. Validation and grid independence test

To evaluate the validity of the simulation, the present results are compared with the results of two articles presented by Refs. [26, 46] The ΔP and HTR reported by Hasan et al. [26] are compared with the present results, as shown in Fig. 2. The results are obtained from the cooling of a pin-fin heatsink with circular pins. The average error between the present results and the ones of reference [26] is 3.47%.

In the validation, the ΔP and the HTR are compared with the experimental results of Horiuchi et al. [46].

Since the grid resolution has a important impact on the results, it is essential to perform the grid independence test. Hence, the results of several meshes are compared when inlet velocity is 1 m/s. The outlet temperature and ΔP are reported in Table 4. As evident, the results do not change when the grid size is 0.0001. Therefore, an unstructured grid is employed to simulate this problem (Fig. 3).

7. Results and discussion

Fig. 4 shows the heatsink temperature for different fins with two arrangements for the blade-shaped nanoparticles and the inlet velocity of 2 m/s. It can be observed that the fluid enters from the top and cools the heatsink. Thus, the inlet section is cooler, and the outlet section is warmer. The sides of the heatsink are warmer due to fluid passage. The fins have a lower temperature in the upper parts due to the cooling fluid flow, while the parts attached to the bottom have a higher temperature due to the application of heat flux from the bottom of the heatsink. The temperature of circular and hexagonal fins is less than that of square and hexagonal ones. The cross section of the fin is much effective in this regard. On the lower part of the heatsink, it can be seen that the parts that have fins have a lower temperature than the side parts, which is due to the conduction heat transfer from the fins to the top.

It seems that as the fluid reaches the fins with different shapes and its velocity in the middle of the fins first increases due to the reduction in the fluid passage, but after passing the first series of fins, its velocity decreases sharply. A significant ΔP occurs due to

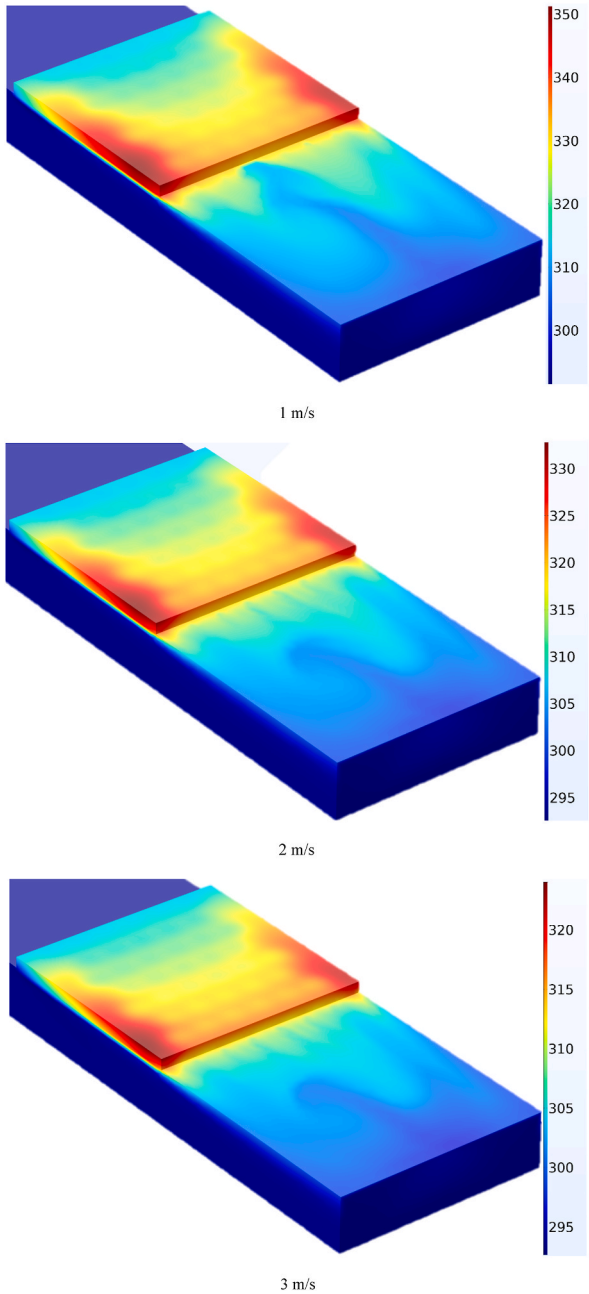

Fig. 5. Temperature contours for different velocities of nanofluid with blade-shaped nanoparticles for ES arrangement of fins.

shear stress created in this area and increases energy losses, leading to a very low magnitude of velocity. The fluid loses its velocity after passing through the heatsink. In some places, the fluid velocity is negative due to the vortex formation, and the fluid flow direction is towards the inlet. The negative pressure in this area causes the fluid to move to the inlet section. Among the different types of fins, square one has a higher ΔP than other types of fins. In the ES arrangement, the fluid accelerates along the walls, and more fluid passes through this area while the other arrangement has less fluid passing through the walls.

The increase in nanofluid velocity at the channel inlet increases the amount of velocity in the whole channel and between the fins. In the three-dimensional case, the fluid is accelerated by reaching the fins at the top. The reason is the narrow passage of the fluid passage in that area. However, the velocity decreases in the middle of the heatsink.

Fig. 5 illustrates the temperature distribution for different velocities of nanofluid with blade-shaped nanoparticles for the ES arrangement of fins. Growing the velocity of the fluid in the channel inlet reduces the maximum temperature, indicating better heatsink cooling performance with higher nanofluid velocities. The increase in the velocity also changes the shape of the vortex after

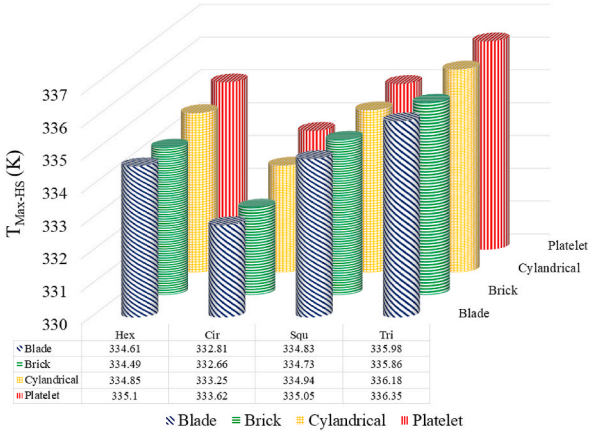

Fig. 6. Maximum heatsink temperature for different types of fins and different nanoparticle shapes for ES model and inlet velocity of 2 m/s.

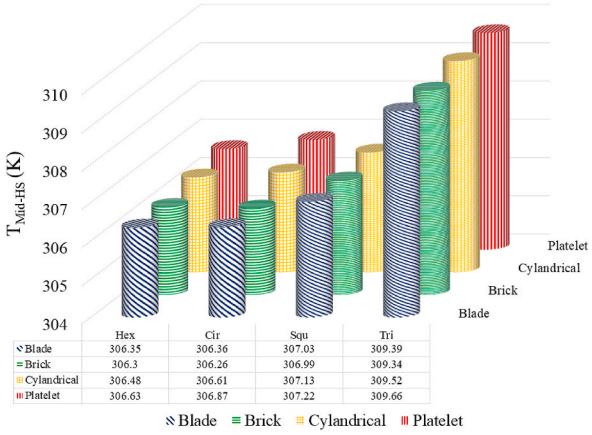

Fig. 7. Heatsink average temperature for different types of fins and different nanoparticle shapes for ES model and inlet velocity of 2 m/s.

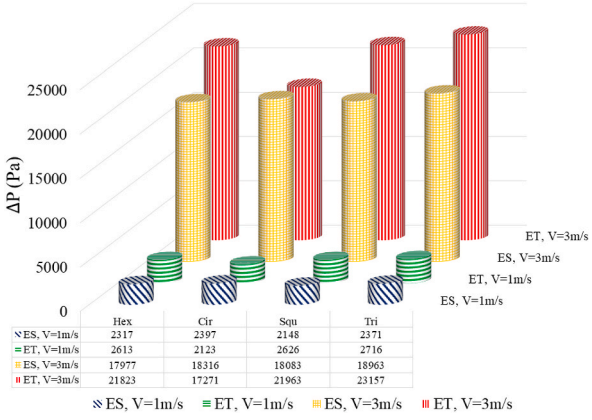

Fig. 8. ΔP at the inlet and outlet of the channel for different types of fins, two velocities, and two arrangements of the fins.

heatsink. As observed, the increase in velocity causes the isothermal plates with lower temperatures to be pulled further to the channel outlet, indicating that the fluid at the outlet has a lower temperature at higher velocities. Increasing the velocity causes the fluid to pass faster over the fins and the hot part, reducing the heat transfer time. As a result, the temperature at the outlet decreases. The highest temperature is seen in the heatsink outlet corner. This part of the fluid has a higher temperature, so it is warmer than other regions.

Fig. 6 shows the maximum heatsink temperature for different types of fins and different nanoparticle shapes for the ES model and inlet velocity of 2 m/s. Among the different fins, circular, hexagonal, square, and triangular, respectively, have the highest temperature. Among the different shapes of nanoparticles, brick-shaped nanoparticles have the lowest maximum temperature. This

nanoparticle has high thermal conductivity, leading to an enhancement in the viscosity slightly, which makes the lowest maximum temperature corresponds to the brick-shaped nanoparticles. The platelet-shaped nanoparticles create the highest temperature in the heatsink. These nanoparticles have the lowest increase in thermal conductivity and give the highest increase in base fluid viscosity.

Fig. 7 shows the heatsink average temperature for different types of fins and different nanoparticle shapes for the ES model and inlet velocity of 2 m/s. As observed, the lowest average temperatures correspond to brick-shaped nanoparticles, which have the highest thermal conductivity and a lower viscosity among other nanoparticles with different shapes. The average temperature is the lowest for circular and hexagonal fins. The triangular fin has a very high average temperature, indicating that the cooling performance of the triangular fins is much weaker than the other ones, which causes the temperature at the ends of the fin to be high.

Fig. 8 shows the ΔP at the inlet and outlet of the channel for different types of fins, two velocities, and two arrangements of the fins. Increasing the velocity causes the amount of shear stress on the solid parts to increase sharply. As a result, the loss increases. Hence, the amount of ΔP is also increased. In the ES model, the square fin causes the minimum amount of ΔP. In the ET model, the circular one leads to the minimum ΔP. The arrangement of the fins causes more or less ΔP for the fins with different shapes. Meanwhile, in both arrangements, the amount of ΔP of the triangular fins is more than other ones.

8. Conclusions

In the present paper, the turbulent flow of alumina nanofluid in a channel with a pin-fin heatsink in the middle of the channel was studied numerically. The nanofluid flow had a velocity range of 1–3 m/s. The fins had different shapes, including hexagonal, circular, square, and triangular, which were placed on the heatsink by two different arrangements. Nanoparticles with different shapes of blade, brick, cylinder, and platelet were considered, and their effect was considered. The main results are as follows:

1 The use of circular and triangular fins creates minimum and maximum temperature in the heatsink, respectively. The use of brick-shaped and platelet-shaped nanoparticles creates minimum and maximum temperatures in the heatsink, respectively.
2 The use of the ET model creates a lower average temperature at high and low velocities compared to the ES model.
3 The use of circular fin requires less ΔP. The use of brick-shaped nanoparticles and platelet-shaped nanoparticles creates minimum and maximum ΔP, respectively.

CRediT authorship contribution statement

Yacine Khetib: Methodology, Writing – original draft. **Khaled Sedraoui:** Conceptualization, Software. **Ammar A. Melaibari:** Review & Editing. **Ali Alzaied:** Validation. **Radi Alsulami:** Review & Editing. **Mohsen Sharifpur:** Review & Editing.

Declaration of competing interest

The authors declare that they have no known competing financial interests or personal relationships that could have appeared to influence the work reported in this paper.

Acknowledgments

“This project was funded by the Deanship of Scientific Research (DSR) at King Abdulaziz University, Jeddah, under grant no. (**RG-11–135–40).** The authors, therefore, acknowledge with thanks DSR technical and financial support”.

References

[1] M. Abedi, D.O. Moskovskikh, A.S. Rogachev, A.S. Mukasyan, Spark plasma sintering of titanium spherical particles, Metall. Mater. Trans. B 47 (5) (2016) 2725–2731, https://doi.org/10.1007/s11663-016-0732-8.
[2] K.V. Kuskov, M. Abedi, D.O. Moskovskikh, I. Serhiienko, A.S. Mukasyan, Comparison of conventional and flash spark plasma sintering of Cu–Cr pseudo-alloys: kinetics, structure, properties, Metals 11 (1) (2021) 141 [Online]. Available: https://www.mdpi.com/2075-4701/11/1/141.
[3] N. Keyvani, A. Azarniya, H.R.M. Hosseini, M. Abedi, D. Moskovskikh, Thermal stability and strain sensitivity of nanostructured aluminum titanate (Al2TiO5), Mater. Chem. Phys. 223 (2019) 202–208, https://doi.org/10.1016/j.matchemphys.2018.10.060.
[4] K.S. Torosyan, A.S. Sedegov, K.V. Kuskov, M. Abedi, D.I. Arkhipov, P.V. Kiryukhantsev-Korneev, S. Vorotilo, D.O. Moskovskikh, A.S. Mukasyan, Reactive, nonreactive, and flash spark plasma sintering of Al2O3/SiC composites—a comparative study, J. Am. Ceram. Soc. 103 (1) (2020) 520–530, https://doi.org/10.1111/jace.16734.
[5] H.E. Ahmed, B.H. Salman, A.S. Kherbeet, M.I. Ahmed, Optimization of thermal design of heat sinks: a review, Int. J. Heat Mass Tran. 118 (2018) 129–153, https://doi.org/10.1016/j.ijheatmasstransfer.2017.10.099.
[6] I.A. Ghani, N.A.C. Sidik, N. Kamaruzaman, Hydrothermal performance of microchannel heat sink: the effect of channel design, Int. J. Heat Mass Tran. 107 (2017) 21–44, https://doi.org/10.1016/j.ijheatmasstransfer.2016.11.031.
[7] S.M. Sohel Murshed, C.A. Nieto de Castro, A critical review of traditional and emerging techniques and fluids for electronics cooling, Renew. Sustain. Energy Rev. 78 (2017) 821–833, https://doi.org/10.1016/j.rser.2017.04.112.
[8] J.F. Tullius, R. Vajtai, Y. Bayazitoglu, A review of cooling in microchannels, Heat Tran. Eng. 32 (7–8) (2011) 527–541, https://doi.org/10.1080/01457632.2010.506390.
[9] M. Afrand, A.H. Pordanjani, S. Aghakhani, H.F. Oztop, N. Abu-Hamdeh, Free convection and entropy generation of a nanofluid in a tilted triangular cavity exposed to a magnetic field with sinusoidal wall temperature distribution considering radiation effects, Int. Commun. Heat Mass Tran. 112 (2020) 104507, https://doi.org/10.1016/j.icheatmasstransfer.2020.104507.

[10] S. Aghakhani, A.H. Pordanjani, M. Afrand, M. Sharifpur, J.P. Meyer, Natural convective heat transfer and entropy generation of alumina/water nanofluid in a tilted enclosure with an elliptic constant temperature: applying magnetic field and radiation effects, Int. J. Mech. Sci. 174 (2020) 105470, https://doi.org/10.1016/j.ijmecsci.2020.105470.
[11] S.-R. Yan, A. Golzar, M. Sharifpur, J.P. Meyer, D.-H. Liu, M. Afrand, Effect of U-shaped absorber tube on thermal-hydraulic performance and efficiency of two-fluid parabolic solar collector containing two-phase hybrid non-Newtonian nanofluids, Int. J. Mech. Sci. 185 (2020) 105832.
[12] S.O. Giwa, M. Sharifpur, J.P. Meyer, Experimental study of thermo-convection performance of hybrid nanofluids of Al2O3-MWCNT/water in a differentially heated square cavity, Int. J. Heat Mass Tran. 148 (2020) 119072.
[13] I.D. Garbadeen, M. Sharifpur, J.M. Slabber, J.P. Meyer, Experimental study on natural convection of MWCNT-water nanofluids in a square enclosure, Int. Commun. Heat Mass Tran. 88 (2017) 1–8.
[14] M. Abedi, D.O. Moskovskikh, A.S. Mukasyan, Reactive flash spark plasma sintering of alumina reinforced by silicon carbide nanocomposites: physicochemical study. Presented at the International Symposium on Self-Propagating High-Temperature Synthesis, XV, Moscow, 2019.
[15] G. Huminic, A. Huminic, Entropy generation of nanofluid and hybrid nanofluid flow in thermal systems: a review, J. Mol. Liq. 302 (2020) 112533, https://doi.org/10.1016/j.molliq.2020.112533.
[16] M.-W. Tian, S. Rostami, S. Aghakhani, A.S. Goldanlou, C. Qi, A techno-economic investigation of 2D and 3D configurations of fins and their effects on heat sink efficiency of MHD hybrid nanofluid with slip and non-slip flow, Int. J. Mech. Sci. 189 (2021) 105975, https://doi.org/10.1016/j.ijmecsci.2020.105975.
[17] S. Sadripour, A.J. Chamkha, The effect of nanoparticle morphology on heat transfer and entropy generation of supported nanofluids in a heat sink solar collector, Thermal Science and Engineering Progress 9 (2019) 266–280, https://doi.org/10.1016/j.tsep.2018.12.002.
[18] A.A. Alfaryjat, A. Dobrovicescu, D. Stanciu, Influence of heat flux and Reynolds number on the entropy generation for different types of nanofluids in a hexagon microchannel heat sink, Chin. J. Chem. Eng. 27 (3) (2019) 501–513, https://doi.org/10.1016/j.cjche.2018.08.009.
[19] A. Shahsavar, M.M. Baseri, A.A.A.A. Al-Rashed, M. Afrand, Numerical investigation of forced convection heat transfer and flow irreversibility in a novel heatsink with helical microchannels working with biologically synthesized water-silver nano-fluid, Int. Commun. Heat Mass Tran. 108 (2019) 104324, https://doi.org/10.1016/j.icheatmasstransfer.2019.104324.
[20] M.W. Alam, S. Bhattacharyya, B. Souayeh, K. Dey, F. Hammami, M. Rahimi-Gorji, R. Biswas, CPU heat sink cooling by triangular shape micro-pin-fin: numerical study, Int. Commun. Heat Mass Tran. 112 (2020) 104455, https://doi.org/10.1016/j.icheatmasstransfer.2019.104455.
[21] Y. Li, L. Gong, M. Xu, Y. Joshi, Hydraulic and thermal performances of metal foam and pin fin hybrid heat sink, Appl. Therm. Eng. 166 (2020) 114665, https://doi.org/10.1016/j.applthermaleng.2019.114665.
[22] Y. Li, L. Gong, M. Xu, Y. Joshi, Enhancing the performance of aluminum foam heat sinks through integrated pin fins, Int. J. Heat Mass Tran. 151 (2020) 119376, https://doi.org/10.1016/j.ijheatmasstransfer.2020.119376.
[23] X. Wang, M. Chen, D. Tate, H. Rahimi, S. Zhang, Numerical investigation on hydraulic and thermal characteristics of micro latticed pin fin in the heat sink, Int. J. Heat Mass Tran. 149 (2020) 119157, https://doi.org/10.1016/j.ijheatmasstransfer.2019.119157.
[24] T. Ambreen, M.-H. Kim, Effect of fin shape on the thermal performance of nanofluid-cooled micro pin-fin heat sinks, Int. J. Heat Mass Tran. 126 (2018) 245–256, https://doi.org/10.1016/j.ijheatmasstransfer.2018.05.164.
[25] B. Abbasipour, B. Niroumand, S.M. Monir Vaghefi, M. Abedi, Tribological behavior of A356−CNT nanocomposites fabricated by various casting techniques, Trans. Nonferrous Metals Soc. China 29 (10) (2019) 1993–2004, https://doi.org/10.1016/S1003-6326(19)65107-1.
[26] M.I. Hasan, Investigation of flow and heat transfer characteristics in micro pin fin heat sink with nanofluid, Appl. Therm. Eng. 63 (2) (2014) 598–607, https://doi.org/10.1016/j.applthermaleng.2013.11.059.
[27] T. Ambreen, A. Saleem, C.W. Park, Pin-fin shape-dependent heat transfer and fluid flow characteristics of water- and nanofluid-cooled micropin-fin heat sinks: square, circular and triangular fin cross-sections, Appl. Therm. Eng. 158 (2019) 113781, https://doi.org/10.1016/j.applthermaleng.2019.113781.
[28] S. Aghakhani, B. Ghasemi, A. Hajatzadeh Pordanjani, S. Wongwises, M. Afrand, Effect of replacing nanofluid instead of water on heat transfer in a channel with extended surfaces under a magnetic field, Int. J. Numer. Methods Heat Fluid Flow 29 (4) (2019) 1249–1271, https://doi.org/10.1108/HFF-06-2018-0277.
[29] A. Hajatzadeh Pordanjani, S. Aghakhani, M. Afrand, B. Mahmoudi, O. Mahian, S. Wongwises, An updated review on application of nanofluids in heat exchangers for saving energy, Energy Convers. Manag. 198 (2019) 111886, https://doi.org/10.1016/j.enconman.2019.111886.
[30] H. Ghodsinezhad, M. Sharifpur, J.P. Meyer, Experimental investigation on cavity flow natural convection of Al2O3–water nanofluids, Int. Commun. Heat Mass Tran. 76 (2016) 316–324.
[31] M. Sharifpur, A.B. Solomon, T.L. Ottermann, J.P. Meyer, Optimum concentration of nanofluids for heat transfer enhancement under cavity flow natural convection with TiO2 – Water, Int. Commun. Heat Mass Tran. 98 (2018) 297–303.
[32] A.A. Awais, M.-H. Kim, Experimental and numerical study on the performance of a minichannel heat sink with different header geometries using nanofluids, Appl. Therm. Eng. 171 (2020) 115125, https://doi.org/10.1016/j.applthermaleng.2020.115125.
[33] Y. Ma, A. Shahsavar, P. Talebizadehsardari, Two-phase mixture simulation of the effect of fin arrangement on first and second law performance of a bifurcation microchannels heatsink operated with biologically prepared water-Ag nanofluid, Int. Commun. Heat Mass Tran. 114 (2020) 104554, https://doi.org/10.1016/j.icheatmasstransfer.2020.104554.
[34] H. Babar, H.M. Ali, Airfoil shaped pin-fin heat sink: potential evaluation of ferric oxide and titania nanofluids, Energy Convers. Manag. 202 (2019) 112194, https://doi.org/10.1016/j.enconman.2019.112194.
[35] S.R. Yan, A.H. Pordanjani, S. Aghakhani, A.S. Goldanlou, M. Afrand, Managment of natural convection of nanofluids inside a square enclosure by different nano powder shapes in presence of Fins with different shapes and magnetic field effect, Adv. Powder Technol. 31 (7) (Jul 2020) 2759–2777, https://doi.org/10.1016/j.apt.2020.05.009.
[36] S.A. Mirmohammadi, M. Behi, Y.X. Gan, L.M. Shen, Particle-shape-, temperature-, and concentration-dependent thermal conductivity and viscosity of nanofluids, Phys. Rev. 99 (4) (Apr 2019), 043109, https://doi.org/10.1103/PhysRevE.99.043109. Art no.
[37] A.H. Pordanjani, S. Aghakhani, Numerical investigation of natural convection and irreversibilities between two inclined concentric cylinders in presence of uniform magnetic field and radiation. Heat Transfer Engineering, 2021, pp. 1–21.
[38] F. Liu, Y. Cai, L. Wang, J. Zhao, Effects of nanoparticle shapes on laminar forced convective heat transfer in curved ducts using two-phase model, Int. J. Heat Mass Tran. 116 (2018) 292–305, https://doi.org/10.1016/j.ijheatmasstransfer.2017.08.097.
[39] H.J. Kim, S.-H. Lee, J.-H. Lee, S.P. Jang, Effect of particle shape on suspension stability and thermal conductivities of water-based bohemite alumina nanofluids, Energy 90 (2015) 1290–1297, https://doi.org/10.1016/j.energy.2015.06.084.
[40] A.A.A. Arani, S. Sadripour, S. Kermani, Nanoparticle shape effects on thermal-hydraulic performance of boehmite alumina nanofluids in a sinusoidal–wavy mini-channel with phase shift and variable wavelength, Int. J. Mech. Sci. 128–129 (2017) 550–563, https://doi.org/10.1016/j.ijmecsci.2017.05.030.
[41] M. Bahiraei, A. Monavari, M. Naseri, H. Moayedi, Irreversibility characteristics of a modified microchannel heat sink operated with nanofluid considering different shapes of nanoparticles, Int. J. Heat Mass Tran. 151 (2020) 119359, https://doi.org/10.1016/j.ijheatmasstransfer.2020.119359.
[42] A. Maji, D. Bhanja, P.K. Patowari, Numerical investigation on heat transfer enhancement of heat sink using perforated pin fins with inline and staggered arrangement, Appl. Therm. Eng. 125 (2017) 596–616, https://doi.org/10.1016/j.applthermaleng.2017.07.053.
[43] H.-C. Chiu, R.-H. Hsieh, K. Wang, J.-H. Jang, C.-R. Yu, The heat transfer characteristics of liquid cooling heat sink with micro pin fins, Int. Commun. Heat Mass Tran. 86 (2017) 174–180, https://doi.org/10.1016/j.icheatmasstransfer.2017.05.027.
[44] A. Sakanova, K.J. Tseng, Comparison of pin-fin and finned shape heat sink for power electronics in future aircraft, Appl. Therm. Eng. 136 (2018) 364–374, https://doi.org/10.1016/j.applthermaleng.2018.03.020.
[45] E.V. Timofeeva, J.L. Routbort, D. Singh, Particle shape effects on thermophysical properties of alumina nanofluids, J. Appl. Phys. 106 (1) (2009), 014304, https://doi.org/10.1063/1.3155999.
[46] K. Horiuchi, A. Nishihara, K. Sugimura, Multi-objective optimization of water-cooled pinfin heatsinks, Int. J. Heat Mass Tran. 81 (2015) 760–766, https://doi.org/10.1016/j.ijheatmasstransfer.2014.10.057.